doi:10.26443/seismica.v4i1.1408

SEISMICA

Monitoring Time Variations in Seismic Noise Amplitude at Permanent Seismic Networks

J. Díaz *[1], **J.A. Jara** [2], **P. Sánchez-Pastor** [1], **T. Frontera** [2], **H. Seivane** [1], **S. Jorde** [1], **Th. Lecocq** [3]

[1]Geosciences Barcelona (GEO3BCN-CSIC), Barcelona, Spain, [2]Institut Cartogràfic i Geològic de Catalunya, Barcelona, Spain, [3]Seismology-Gravimetry, Royal Observatory of Belgium, Brussels, Belgium.

Author contributions: *Conceptualization*: J. Diaz. *Data Curation*: J.A. Jara, T. Frontera. *Funding Acquisition*: A. Thirdauthor. *Investigation*: J. Díaz, P. Sánchez-Pastor, H. Seivane, S. Jorde, J.A Jara. *Methodology*: J. Diaz, Th. Lecocq. *Software*: Th. Lecocq. *Validation*: P. Sánchez-Pastor, H. Seivane, S. Jorde. *Visualization*: J. Diaz. *Writing – original draft*: J. Diaz. *Writing – review & editing*: J. Díaz, J.A. Jara, P. Sánchez-Pastor, T. Frontera, H. Seivane, S. Jorde, Th. Lecocq.

Abstract The quality control process usually followed at broad-band seismic networks includes the calculation of the power spectral density and their probability density functions. These results do not make possible a quick estimation of temporal variations that can result from non-continuous sources of noise, meteorologic phenomena, etc. We propose the use of the SeismoRMS package, originally developed to analyze the seismic amplitude variations associated with the COVID19 lockdown, to monitor the time evolution of seismic noise sources in a permanent network, using as a case example the dataset collected during 2023 by the CA network in NE Iberia. Frequencies above 1 Hz show remarkable differences between the stations, despite sharing similar installation settings. Most of the sites show day/night and working day/weekend variations, suggesting a relevant contribution of anthropic sources, but the amplitude of such variations differs strongly among the sites. Our study allows us to identify specific sources of noise affecting some sites during short and regular time periods, an aspect that needs to be taken into account when evaluating the overall quality of each site. We conclude that a systematic analysis of the amplitude variations at different frequency bands can be a tool of interest for the management of a broad-band seismic network.

Production Editor:
Gareth Funning
Handling Editor:
Atalay Ayele
Copy & Layout Editor:
Aisling O'Kane

Signed reviewer(s):
Ryan Gallacher
Johannes Schweitzer

Received:
July 27, 2024
Accepted:
February 28, 2025
Published:
April 7, 2025

1 Introduction

Seismic noise is used in different ways in the context of permanent seismic network management. Prior to the final site selection, seismic noise is often used to calculate Horizontal to Vertical Spectral Ratio (HVSR) (Nakamura, 1989) and V_{30} models (e.g., Alexopoulos et al., 2023). The analysis of these results makes it possible to choose the best option, in terms of site amplification, to finally install a permanent station. Once the stations are operational, quality checking of permanent seismic stations typically includes the evaluation of Power Spectral Density (PSD) and Probability Density Functions (PDF), that are used to build station book files, such as those used in the European Integrated Data Archive (EIDA) standards. PSD integrating data from several days/months is a reasonable quantification of the noise levels at a site. PDFs allow the user to evaluate the dominant power amplitude for each period and allow the noise level comparison at each station with reference to Peterson (1993)'s new high noise model (NHNM) and new low noise model (NLNM). These results provide a good characterization of the mean noise levels as a function of frequency for each specific site, but offer a static view of noise distribution. Even if they can be recalculated at regular intervals, they do not allow the user to easily evaluate temporal changes that can result from electronic problems, tilting and/or deformation or changes in the location of local sources of vibration.

In this contribution, we propose the use of an open-access software package originally developed to analyze the seismic amplitude variations associated with the COVID19 lockdown, as a monitoring tool of the temporal evolution of the sources of seismic noise for a permanent seismic network at selected frequency bands. As an example, we have analyzed a full year of data (1/1/2023-31/12/2023) from broad-band stations of the ICGC network, covering the Catalonia region in NE Iberia and identified with the CA code (Institut Cartogràfic i Geològic de Catalunya, 1984). Knowing the time variations of noise sources that affect the stations at different frequency bands can be useful, as an example, to interpretate correctly the differences in the detection level that may arise during a seismic crisis. These differences may be due to structural changes in the rupture process, but they also can be related to large background noise energy during working times at some stations. Our objective is not to provide a detailed report of the noise sources for each station, but to demonstrate the potential of the proposed approach to control the eventual time changes in the noise levels at permanent seismic networks.

*Corresponding author: jdiaz@geo3bcn.csic.es

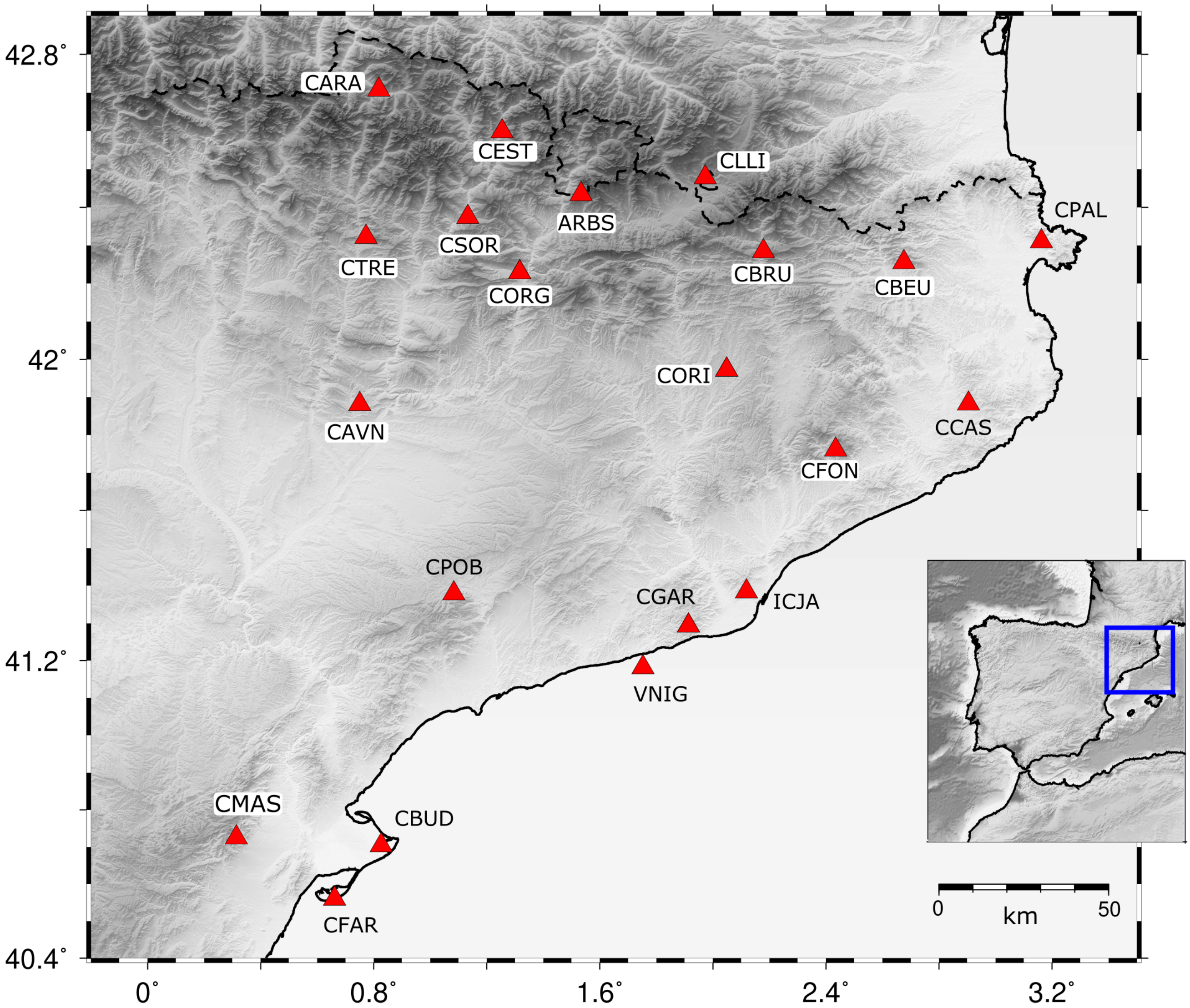

Figure 1 Location of the CA broad-band seismic network covering NE Iberia.

2 Data and Method

The ICGC seismic network was created in the late 1980s and covers the Catalonia region in NE Iberia (Figure 1). Its aim is to provide high quality, open-access seismic data to the scientific community and to civil protection services, hence densifying the data collected by the Spanish national seismic network. Following successive upgrades, the network is now composed of up to 21 broad-band open access stations, covering NE Iberia, but sampling more densely the areas with more seismic activity, the Pyrenees to the north and the Mediterranean coast to the east. One of the stations has been excluded from our analysis, as it presented technical problems during a large part of 2023, making it difficult to compare its results with the rest of the network. The network includes two special sites not following the standards, a permanent ocean bottom seismometer (VNIG) located near the coast, 30 km south of Barcelona, and a broad-band station located in the center of Barcelona (ICJA). Additionally, 26 accelerometers have been installed over the last few years, mostly located in urban areas, to record large magnitude events which could affect the region. Seismic data of the CA network is publicly available using the fdsnws server maintained by ICGC (http://ws.icgc.ca/fdsnws) or using the distribution services offered by ORFEUS EIDA (http://www.orfeus-eu.org/data/eida/) and FDSN (https://www.fdsn.org/services/) data services.

The SeismoRMS software package (Lecocq et al., 2020) was designed to analyze changes in the seismic noise due to the reduction of human activity resulting from the COVID19-related lockdown measures adopted by the civil authorities all around the world. We propose here to use this software, available open access through GitHub, to evaluate the seismic noise time evolution in different frequency bands for all the broad-band stations of a permanent seismic network.

The SeismoRMS is written in Python and based on the use of the routines integrated in the Obspy package (Krischer et al., 2015). Its key point is the computation, storage, and graphic representation of time variations of the seismic background noise ground

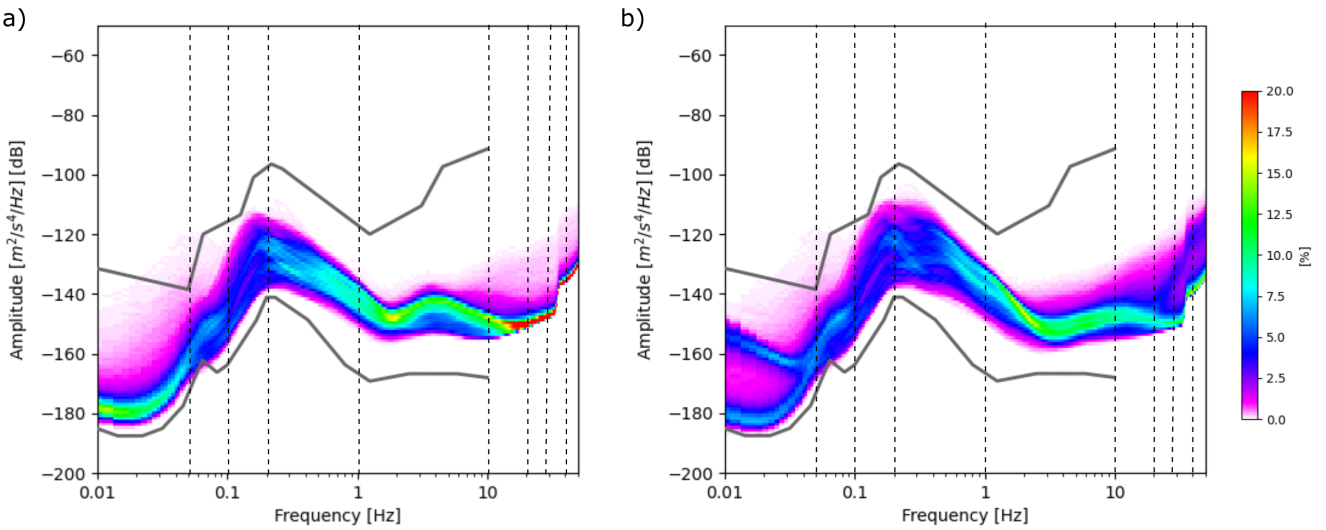

Figure 2 PDF of the PSD for stations CA.CARA.HHZ (a) and CA.CBRU.HHZ (b). Vertical dashed bars show the frequency intervals chosen in our analysis. Grey lines show the NHNM and the NLNM models (Peterson, 1993).

motion acceleration at specific frequency bands. The software has been designed to be easy and fast to use and allows the user to visualize the time variations of amplitude using different graphics.

In the first stage, data is downloaded from a fdsnws server on a daily basis and the instrument response, also retrieved from the fdsnws server, is removed using the Obspy routines. In this study we have focused only on the vertical components of the seismic signal. Secondly, the data is divided into 30-minute-long windows with an overlap of 50% and the power spectral density of each segment is calculated using the Welch method (Welch, 1967). This approach reduces noise in the power spectra, although it also results in a reduction of the frequency resolution, which is minimized with a robust smoothing parametrization. PSDs are calculated on a daily basis, taking into account assuring the continuity between successive days by including overlapping windows, and stored as numpy arrays using the npz compressed format in order to be quickly accessible for further analysis and to facilitate the addition of new data.

The resulting PSDs can be represented in terms of power of the seismic acceleration, expressed in decibels (dB) and referred to 1 $m^2/s^4/Hz$. Following a classical approach, the results are displayed in form of power density functions (Figure 2), where the color palette indicates the probability of a given amplitude for each frequency value. This approach facilitates the comparison with the new high-noise model and the new low-noise model (Peterson, 1993). As observed in Figure 2, some stations have a PDF with a clearly defined most probable amplitude at each frequency (CARA, Figure 2a), while others show two different preferred amplitude levels, in particular at low frequencies and near the microseismic peak (CBRU, Figure 2b). As discussed later, this is an indicator of systematic time variations in the level of background noise.

The SeismoRMS package makes it possible to calculate the root mean square (RMS) of the seismic noise amplitude for any frequency band of interest. It also provides an easy way to graphically represent the time evolution of the seismic amplitudes, based on the use of Matplotlib routines (Figure 3). Aspects such as seasonal changes, amplitude peaks at specific hours of the day or night/day and working day/weekend variations can be analyzed in detail using the different outputs of the program. As an example, Figure 3a shows the variations of averaged power amplitude, Figure 3b evidences the lower amplitudes during the weekend and Figures 3c and 3d show the difference between daytime and nighttime or the change between the winter and summer official times, on March 26 and October 28, 2023. The availability of the python codes enables to adapt such images to specific needs of the user.

3 Selection of the frequency bands of interest

In order to evaluate the time variation of the seismic noise amplitude over time, it is convenient to analyze different frequency bands separately, an option easily provided by the software. We have decided to inspect nine different frequency bands, ranging from 10 mHz to the maximum frequency allowed by the data sampling, 50 Hz.

Regarding long periods, we have selected the 10 – 50 mHz frequency band, located below the microseismic peak and usually interpreted as dominated by the Earth's hum. Next, we focus on the single frequency (SF) or primary microseismic (PM) peak, located between 0.05 and 0.1 Hz, with a maximum close to 0.07 Hz. This peak, corresponding to the frequency of oceanic gravity waves in open waters, is observed worldwide and its origin is related to direct pressure fluctuations at the ocean bottom from breaking and/or shoaling waves, generally in shallow waters (Hasselmann, 1963). The double frequency (DF) or

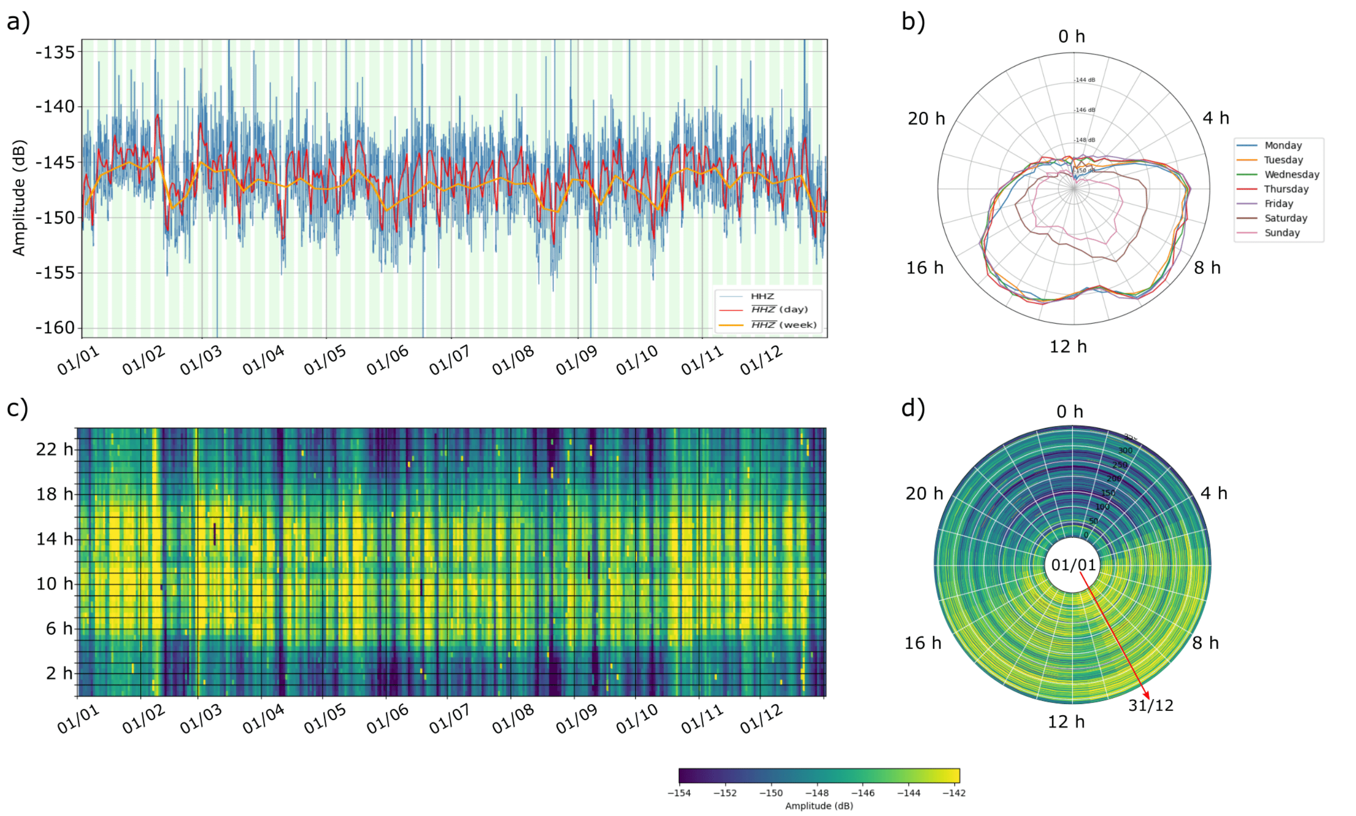

Figure 3 Graphical representations of the time variations of the power of the seismic acceleration amplitude for the 1.0-10.0 Hz frequency band at station CCAS. Power amplitudes are expressed in dB, relative to 1 $m^2/s^4/Hz$. (a) RMS of the power amplitude calculated every 30 minutes (blue line), averaged daily (red line) and averaged weekly (orange line). (b) Power amplitude variation averaged for each day of the week and represented as a function of the hour of the day. (c) Power amplitude variation, represented using a color palette, as a function of the hour of the day. (d) Idem, but represented in a circular graph.

secondary microseismic (SM) peak, extending between 0.1 and 1 Hz, includes most of the seismic energy recorded in the absence of large earthquakes. Its origin is related to the interaction of oceanic waves traveling in opposite directions and generating stationary waves with a frequency peak near 0.14 Hz, twice the ocean wave frequency (Longuet-Higgins, 1950). Several authors have proposed a subdivision of the secondary peak into two bands; between 0.1 and 0.2 Hz the origin has been related to storms impacting large sections of the coastline, while for frequencies above 0.2 Hz the origin is related to the local sea state and it is often correlated with local wind speed (Bromirski et al., 2005; Díaz, 2016; Stephen et al., 2003). Recently, Wilgus et al. (2024) have pointed out that the power levels in the 0.3-1.3 Hz band decay as a function of proximity to the coastline, probing that a reduction of 25 dB can be achieved by installing the seismometer 25 km away from the shoreline. To take these points into consideration, we decided to explore the 0.1-0.2 Hz and 0.2-1.0 Hz bands separately.

For frequencies above 1 Hz, the seismic records in absence of waves generated by earthquakes are dominated by natural sources, including wind, rainfall, river discharges or sonic waves generated by thunders, and by human-generated vibrations, including moving vehicles, trains, citizen activities, etc. Different authors have shown that the anthropogenic contribution is usually larger at frequencies between 1 and 30 Hz. It has also been shown that intense rainfall associated with storms can significantly contribute to the seismic amplitudes for frequencies above 40 Hz (Diaz et al., 2023). Therefore, we decided to analyze the noise variations in 10 Hz wide frequency bands: 1-10, 10-20, 20-30, 30-40 and 40-50 Hz. As most of the stations provide sampling of 100 sps, the last band was limited to 40-47 Hz to avoid problems with the aliasing frequency.

4 General trends in the seismic noise amplitude variations

Figure 4 shows the daily power amplitude variation for station CAVN, located in a monastery far from areas with important anthropogenic activity. Power amplitude values for each frequency band are calculated every 30 minutes, averaged for 12 h intervals and represented using a common amplitude scale. Although more details on the amplitude variation over time will be provided in the next section, this figure illustrates the strong differences between the time variation patterns for frequencies above and below 1 Hz.

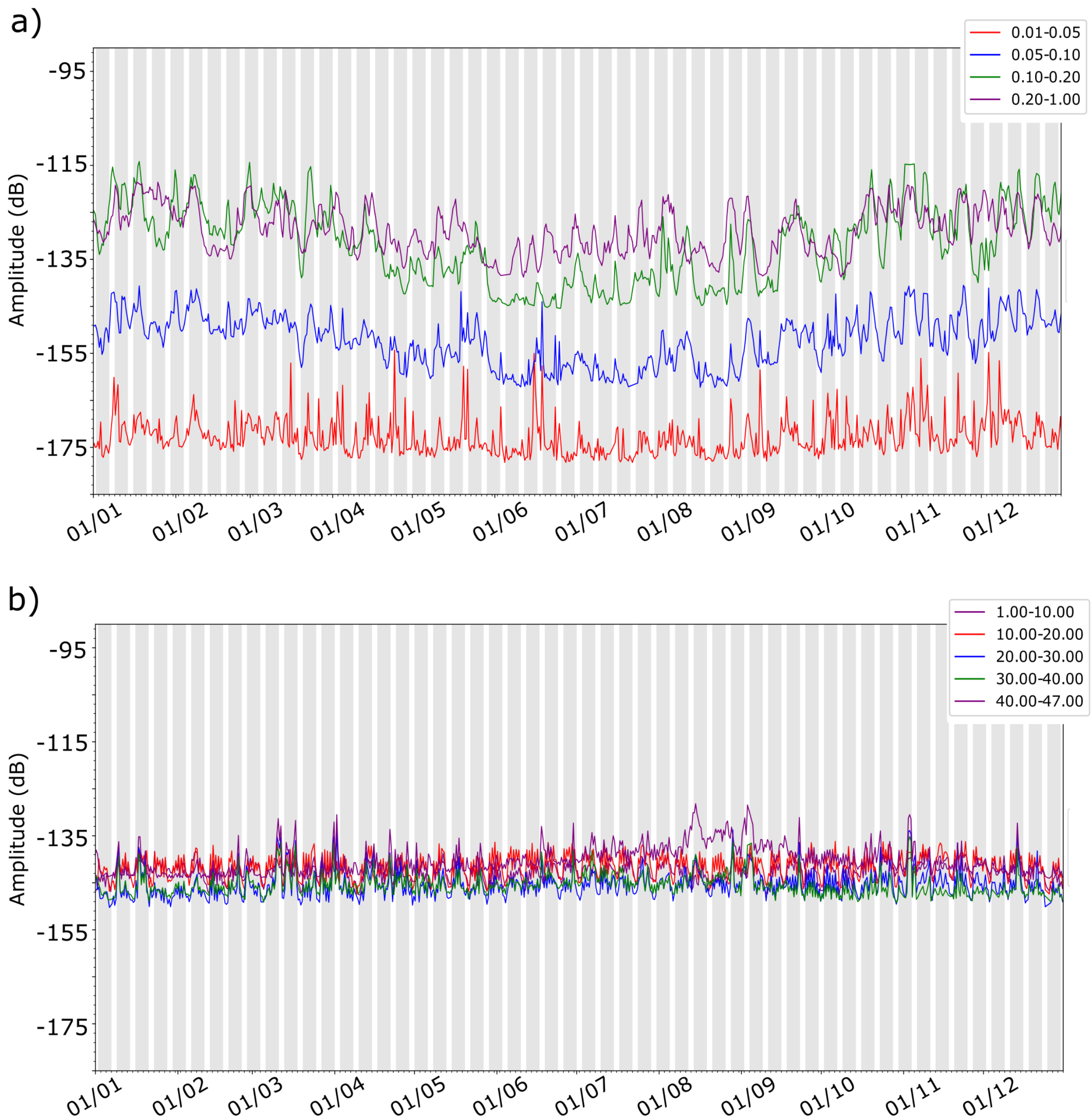

Figure 4 Mean amplitude values for station CAVN at the analyzed frequency bands. Upper panel: Frequency bands below 1 Hz. Lower panel: Frequency bands above 1 Hz. Mean values calculated in 12 hours intervals.

Low frequency bands show very similar temporal variation patterns, slightly different for the upper part of the SM (0.2-1.0 Hz). On the contrary, the amplitudes at each band strongly differ, with the lowermost band reaching minimum values below -175 dB, while the PM reaches values around -155 dB and the SM -135 dB. The relative value of these amplitudes shows a clear difference between summer and winter months, discussed in detail in Section 5.1. These results are similar for all the stations of the CA network (Supplementary Figures 1-5).

Regarding frequencies above 1 Hz, all the frequency bands show similar time variation and amplitude values, ranging from -135 to -150 dB, except for a period of four weeks between August and September, in which the 40-47 Hz band evolves differently for this particular station. As discussed in detail in the next section, this pattern of amplitude variation is generally dominated by the day/night and working day/weekend cycles, although large relevant differences do appear among the stations of the network.

This notorious difference between the noise amplitude variation patterns above and below 1 Hz is better imaged representing the amplitude variations as a function of the hour of day, as shown in Figure 5, corresponding to station CORI, located in a relatively low populated area in central Catalonia. For frequencies below 1 Hz, the amplitudes are dominated by seasonal changes, with greenish colors, representing high amplitude values during the winter period. At frequencies above 1 Hz, the most evident variation is related to night/day variations, with greenish colors indicating the working hours of each day. This amplitude variation is particularly marked for the 10-20 Hz and 20-30 Hz ranges, and decreases for the highest frequencies analyzed.

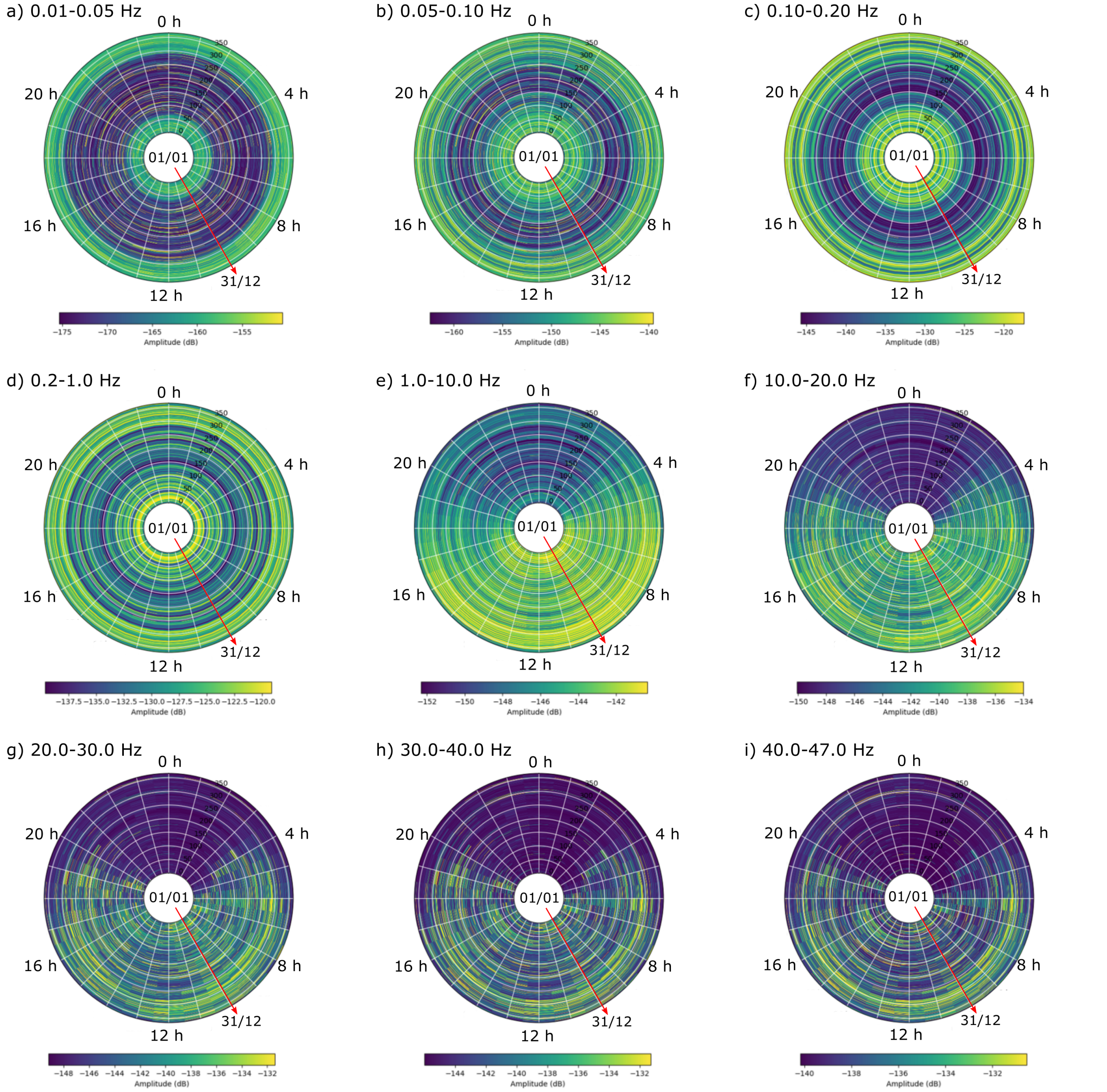

Figure 5 Power amplitude variations over time, as a function of the hour of the day for the different bands analyzed for station CORI. The inner circle correspond to 1st January 2023 and the outer circle shows results for 31 December.

5 Comparing the frequency content of the seismic network stations

As stated in the introduction, the main goal of this contribution is to show how the analysis of the amplitude variations at different frequencies can contribute to a better management of permanent seismic networks. We will first describe the features observed at the different frequency bands and then focus on some stations with anomalous features, trying to understand the local sources of noise affecting these sites.

5.1 Frequencies below 1 Hz

Figure 6 shows examples of the power amplitude variations at three stations covering different zones of the territory for the frequency bands below 1 Hz. Supplementary Figures 6-12 present the same information for all the stations of the network.

The 10-50 mHz frequency band shows high uniformity throughout the year for many of the stations. However, eight of them show an amplitude difference between summer and winter months, with lowest values between mid-March and October: Some of these stations, including CBUD, CFAR, CMAS, and less clearly, CSOR, show two high-amplitude time

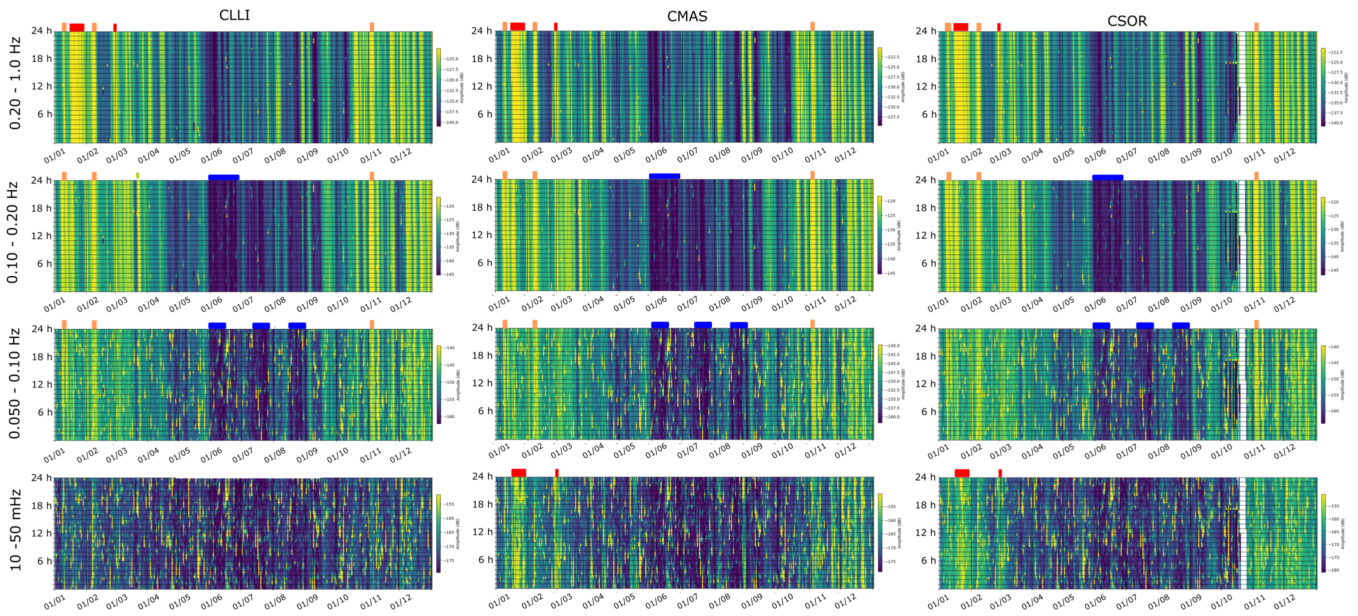

Figure 6 Power amplitude variations at low frequency bands as a function of the date and time of day for three stations covering different geographical zones (see Figure 1). Red boxes highlight time periods with high amplitudes at the 0.2-1.0 Hz and 10-50 mHz bands. Orange boxes show high amplitude intervals at the PM and SM bands and blue boxes show low amplitude time intervals.

intervals, in late January and early March, marked with red boxes in Figure 6. As an example, the daily mean values during these time intervals are around -155 dB for CMAS and CSOR, in contrast with values around -175 dB during summer time. As discussed further below, the 0.2-1.0 Hz band also shows high amplitudes during the same time periods, while the intermediary bands show a different pattern.

The frequency band including the primary microseismic peak (0.05-0.1 Hz) shows, as expected, a clear seasonal variation for almost all the stations, with a low level of noise from June to late August, including three time intervals with even lower amplitudes in early June, mid-July, and mid-August (blue boxes in Figure 6), during which the daily amplitude values reach -160 dB. Time intervals with consistent high levels of noise, including in early January, early February, and early November, can also be identified at most stations, and are highlighted with orange boxes in Figure 6 reaching values close to -140 dB. These episodes are not identified in the 10-50 mHz band. The only exception to this amplitude variation pattern is ICJA, located within Barcelona city and affected by leakage currents from the metro and tramway systems (Díaz et al., 2020).

The 0.1-0.2 Hz frequency band, including the lower part of the SM, also shows a very similar variation pattern for all the stations, including in this case ICJA. The transitions between time intervals with high and low levels of amplitude are here sharper than for the PM band. Although amplitudes are low from mid-April to early October, the time interval with minimum amplitudes is detected in June, with daily mean amplitudes around -145 dB (blue box in Figure 6). The time intervals with high levels of amplitude, such as those in early January, early February, and early November, coincide with those observed in the PM band, suggesting a common origin of the signal. In the 0.1-0.2 Hz band, the daily mean amplitudes during these noisy time intervals reach values as high as -115 dB. The general coincidence during the time intervals with intermediate amplitudes (April-May, November-December) is also consistent with this hypothesis. However, some differences can be identified in the low amplitude season. While the June amplitude minimum is better detected here, the PM band better delineates the low amplitude time intervals in mid-July and mid-August.

Moving to the upper part of the SM band, between 0.2 and 1.0 Hz, all the stations show a similar pattern of amplitude variations, with a clear seasonal variation. However, the amplitude variation pattern is significantly different than in the PM and lower SM bands. In particular, the extended time intervals with low amplitude observed in the 0.1-0.2 Hz cannot be identified here, where the episodes of similar amplitudes are shorter and rarely exceed a few days. Another significant difference involves the high noise period (-120 dB) in middle January, not observed in the 0.1-0.2 and 0.05-0.1 Hz bands, but coincident with the high amplitude period identified at some stations in the 10-50 mHz band (red boxes in Figure 6). It is also important to note that the similarity among the stations is clearly lower in this frequency band. This seems to confirm a different origin for the lower and upper part of the SM, with frequencies above 0.2 Hz dominated by near coastal effects, as proposed by Wilgus et al. (2024). However, contributions from local winds can not be ruled out, so further inspection of the data over specific time intervals will be necessary to confirm this hypothesis.

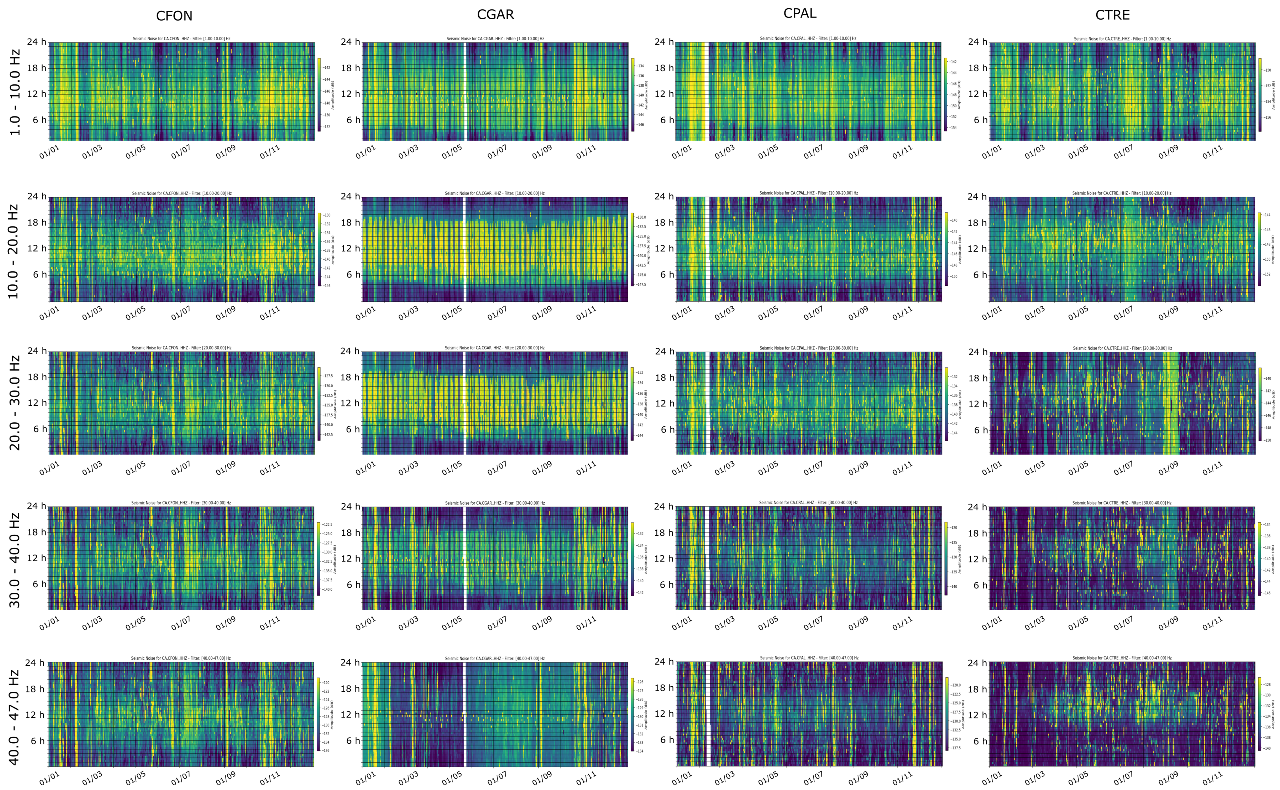

Figure 7 Comparison of the power amplitude variations at high frequencies for three representative stations.

5.2 Frequencies above 1 Hz

Frequencies above 1 Hz show less differences in the absolute amplitude values, but much more differences in their time variability. We show the amplitude variations at these frequency bands for four representative stations in Figure 7. Supplementary Figures 13-19 show the results for the whole network.

It is well-known that seismic amplitudes at frequencies above 1 Hz are strongly influenced by anthropogenic sources (e.g. Díaz, 2016). Although the CA permanent network has its seismometers installed in dedicated vaults located in selected places far from towns and roads, the standard quality checking procedure has evidenced that some of the sites are affected by human-related vibration sources.

The 1-10 Hz frequency band can be interpreted as a transition zone in which the effects of natural and anthropogenic sources have a similar contribution to the seismic amplitudes. As observed in Figure 7, this frequency band shows a certain degree of seasonality, with higher amplitudes generally recorded during winter months. Although there are relevant differences among stations, daily mean amplitude difference between winter and summer in this band is around 4 dB. Most of the stations consistently record common features, such as the time intervals with low amplitudes in late February, early June, late August, or early October. Features observed in the upper SM band, as the high amplitude interval in late January, can also be identified here, suggesting that they are related to natural sources affecting the whole region covered by the network. On the other hand, most of the stations show day/night – working days/weekend variations reaching up to 8 dB, more clearly seen at CARA, CAVN, CBEU, CCAS, CGAR, CLLI, CORG, CORI and ICJA, clearly pointing to a significant contribution of anthropic sources.

The 10-20 Hz, 20-30 Hz and 30-40 bands share many characteristics, with no seasonal variations or time intervals with low or high amplitude observed consistently at several stations. This lack of consistency among the stations suggests that the contribution of sources of vibration located near the seismometers becomes more important as frequency increases. For most of the stations, the day/night and working day/weekend variability decreases with frequency, as can be observed, for example at CGAR (Figure 7). The most prominent effect of anthropogenic sources is therefore observed in the 10-20 Hz band. Moving to the highest frequencies analyzed (40-47 Hz), the results are similar, without seasonal variations or clear indicators of anthropic sources. However, many stations (as CFON and CPAL in Figure 7) show amplitude levels of a few dB higher during daylight hours, a pattern of variation consistent with wind-generated vibrations, which tend to be stronger during the day (e.g. Ashkenazy and Yizhaq, 2023) and mainly affect frequencies above 40-60 Hz (Rindraharisaona et al., 2022).

Amplitude variations related to anthropogenic sources can be analyzed in more detail using graphics presenting the amplitude variations over the entire investigated time interval, averaged for each day of the week. Figure 8 shows the results for the 10-20 Hz band, with each station normalized to its minimum/maximum values. Supplementary Figures

20-24 show the results for the 1-10, 10-20, 20-30, 30-40 and 40-47 Hz bands.

All the stations experience higher levels of noise during daylight hours, with differences reaching 8-10 dB in some cases. The high amplitude period usually starts around 05:30-06:00 UTC, although some stations start earlier (CAVN, 05:00 UTC) or later (ARBS, 09:00 UTC). In the afternoon, most of the sites show a clear decrease in the amplitudes starting around 18:00 / 19:00 UTC.

The most useful information provided by this representation is the clear observation of the difference in amplitudes between working days, Saturdays and Sundays, a feature that denotes a relevant contribution of anthropogenic sources. We can identify that stations such as ARBS, CBRU, CBUD, CFAR, CFON, CMAS and CSOR are less influenced by nearby human activity, as shown by the similar amplitude values recorded during working days and weekends. Stations such as CARA or CORI show a certain lowering of the noise levels during the weekends, while others, such as CAVN, CBEU, CCAS, CGAR, CORG, CPAL, CTRE or ICJA show a strong variation, reaching 3 dB for CCAS or 8 dB in the case of CGAR. For these cases, noise is lower on Sundays and the difference between Sunday and Saturday is larger in morning hours. At highest frequencies, the differences between working days and weekends tend to vanish, with the exception of ICJA, clearly affected by the vibrations induced by city traffic and subway activity.

5.3 Detecting anomalous features at specific stations

The ambient noise amplitude variation analysis presented here is an excellent tool to identify and characterize stations with anomalous background noise. A more detailed description of the variable noise sources for each of the stations of the network is beyond the scope of the study. However, we think that it can be illustrative to the reader to show some specific features observed in our dataset.

While most stations have mean amplitude values around -135 / -150 dB for frequencies above 1 Hz (Supplementary Figures 1-5), CFAR and CBUD have a higher noise level, ranging from -130 to -100 dB, probably due to their location in the Ebro River delta, an area with unconsolidated sediments very close to the seashore (Figure 9a). However, each of these two stations has a clearly different variation pattern. The 1-10 Hz band in CFAR is affected by increased levels of noise from mid-September to October 15, which are not clearly observed at CBUD and extend to the 20-30 Hz band. High amplitudes reaching -92 dB are observed from 06:30 to 17:30 official time, with a break between 12:30 and 13:30 (Figure 10a). This pattern strongly suggests that these vibrations are due to human activity and, more specifically, to the activity in a marine salt exploitation plant located around 3 km away from CFAR. We have verified that the peak of activity in this plant, corresponding to the recollection and processing of the salt, does occur during early fall, hence significantly increasing the noise at this site. A less energetic episode of high noise with similar characteristics can be identified between mid-January and the end of February and seems to be related to a time interval of lower activity in the salt exploitation site.

ICJA station, located within the city of Barcelona, shows, at frequencies above 1 Hz, a strong day/night and working day/weekend variability, with differences exceeding 10 dB between day and night intervals and reaching 5 dB between working days and weekends (Figure 9b). As analyzed previously (Díaz et al., 2017), this signal is mostly due to traffic and subway activity. However, data from 2023 shows an interesting point. Starting June 26, the diurnal amplitude level suddenly increases around 4 dB, in particular in the 1-10 Hz band. This change in the background noise properties is probably related to the demolition and rebuilding works at the FC Barcelona stadium, located 500 m away from the seismic station, which began at the end of June. The lower amplitude observed from the end of June between 13:00 and 14:30 official time would correspond to the lunch break at the construction site.

Notably, at higher frequencies the change in amplitude is less clear and the midday break-off cannot be identified. This suggests that the high frequency vibrations related to this civil work attenuate quickly and hence do not affect frequencies above 20 Hz. The lower panel in Figure 9b evidences that a similar amplitude increase is observed at frequencies as low as 10-50 mHz. Modern broad-band sensors measure the voltage required to counteract the effect of ground motion on a reference mass, keeping it static. It has been proposed that strong variations in the local electromagnetic field can generate currents that interfere with these values, generating signals not related to ground motion (e.g., Díaz et al., 2020; Kozlovskaya and Kozlovsky, 2012). The abrupt increase in late June, at the time period when the civil works at the FC Barcelona stadium started, suggests that these works could generate leaking currents transmitting in the soil and perturbing the seismometer detection system at very low frequencies. However, further investigation will be needed to confirm or disprove this hypothesis.

As an example of short lasting features which can also be detected using SeismoRMS, Figure 9c (upper panel) shows that CFON has increased amplitudes around 06:30 UTC every Tuesday and Wednesday. The signal content extends from 1 to 30 Hz, with maximum expression in the 10-20 Hz band. To better identify the characteristics of this signal, we have extracted the waveforms corresponding to 5 successive Tuesdays (Figure 9c, lower panel). The signal does not occur at the same hour every time and has a duration close to one minute. The CFON seismic station is located in a quiet mountain area, at 300m from a building hosting services from the Montseny mountain park office. This anomalous signal detected at similar times two days per week seems to correspond to a car regularly arriving at these offices. As the background energy at this band is low, our analysis can detect this particular kind of regular-occurring, transient source of noise.

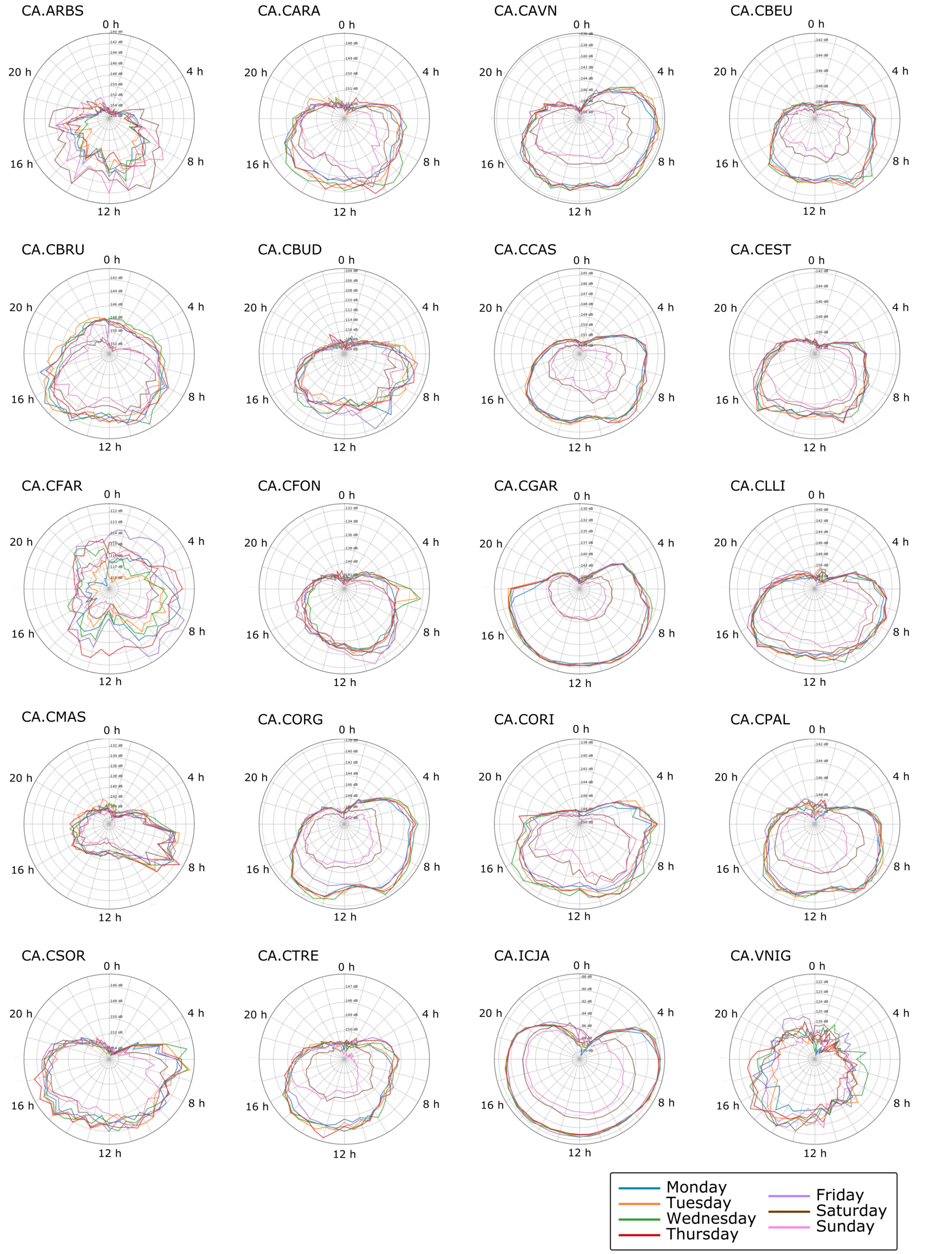

Figure 8 Power amplitude for the 10-20 Hz frequency band, represented as a function of the hour of the day and the day of the week. Each line, represented with different colors, shows the mean values for the days of the week (Monday-Sunday).

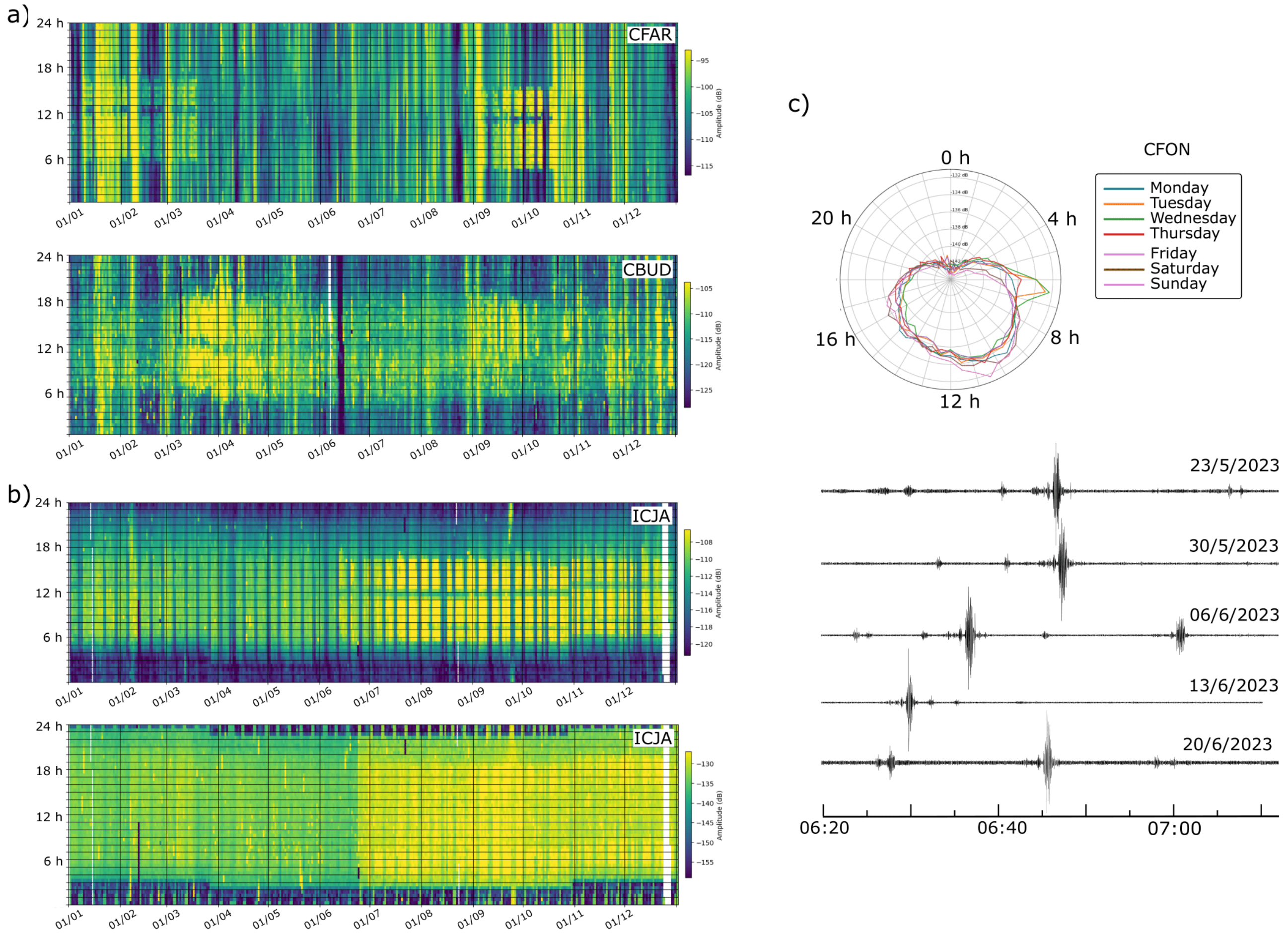

Figure 9 (a) Identification of anthropogenic noise at CFAR and CBUD (1-10 Hz). (b) Increase in the background energy at station ICJA in the 1-10 Hz band, related to the beginning of the demolition and rebuilding works at the FC Barcelona stadium (upper panel). Coincident increase in background energy a the 10-50 mHz band (lower panel). (c) Identification of an early morning amplitude peak on Tuesday/Wednesday at CFON. Upper panel shows the power amplitude for the 10-20 Hz band, represented as a function of the hour of the day and the day of the week. Lower panel shows the waveforms for 5 successive Tuesdays, filtered between 10 and 20 Hz.

6 Discussion and Conclusions

In order to discuss and summarize the obtained results, Figure 10 shows the normalized displacement amplitude throughout the entire 2023 year for all the stations of the CA broad-band network, with each line corresponding to one station and lighter colors indicating larger values of amplitude.

The first observation is that for frequencies beneath 1 Hz, the time intervals with different amplitude levels are consistent among the whole network, while for frequencies above 1 Hz, there is more scattering. On the contrary, the amplitude values at each station are rather uniform at high frequencies, but show larger variations at lower frequencies.

There are three stations in the CA network that have a clearly distinct background noise pattern. The ICJA broad-band station, installed in the basement of the GEO3BCN institute in central Barcelona and originally devoted to outreach activities, shows the largest amplitude values, both at high frequencies and at frequencies below 0.05 Hz. However, the amplitudes in the microseismic peak range do not differ from those in stations which are located in quiet environments. Stations CBUD and CFAR, both located in the Ebro River delta, over unconsolidated sediments and close to the seashore, also show anomalous amplitude values, in particular at low frequencies. In this case, the larger than usual amplitude level can be identified in the PM band and less clearly in the SM peak bands. Another special case is the VNIG ocean bottom seismometer, installed near the coast, 40 km south of Barcelona. Although technical problems during 2023 have resulted in a discontinuous dataset, the available results are consistent with the neighboring stations.

The similarity of the amplitude variation pattern within the PM and SM bands confirms that the origin of the background is mostly related to oceanic waves. The amplitude at these lower frequencies does not show daily or weekly regularity, indicating that the seismic noise in this band is not influenced by human activity.

Our results also confirm that the upper and lower parts of the SM have different properties; while frequencies between 0.1 and 0.2 Hz show amplitude

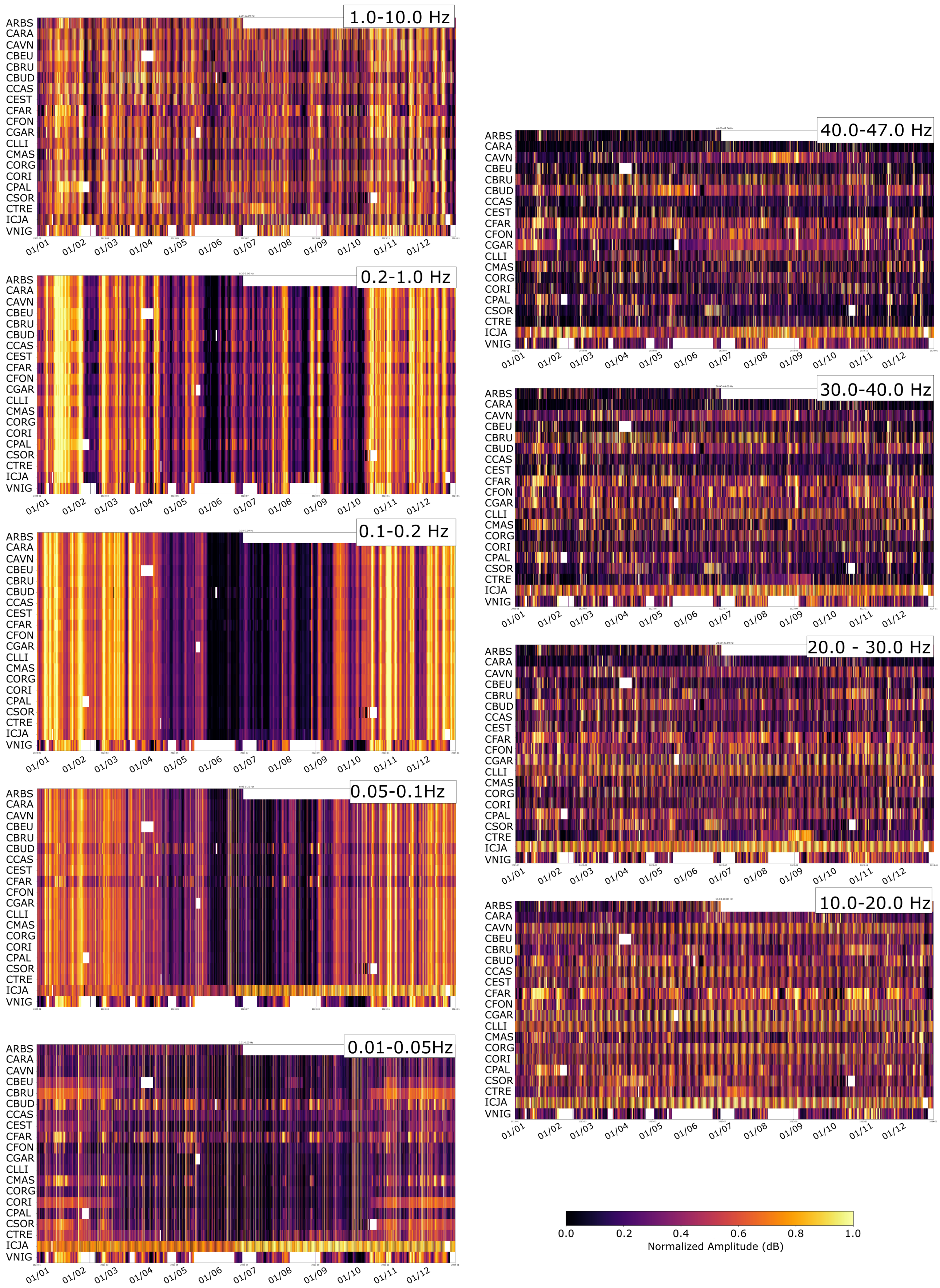

Figure 10 Hourly means of the power amplitude at the different frequency bands, normalized to percentage variation of the baseline, with light colors representing the highest amplitude values.

variations very similar to those in the PM band, the frequency range from 0.2 to 1.0 Hz follows a different pattern. A number of stations show coetaneous high amplitude time intervals in the upper SM band and the 0.010 -0.050 Hz band, but not in the lower SM and the PM bands. This is consistent with the classical hypothesis of an open water origin for SM and suggests that the Earth's hum can have a similar origin, at least partially. The strong seasonality observed in the PM and lower SM bands argues in favor of this origin, as it may be explained by the lower level of wave breakings near the shore during summer.

The 1-10 Hz band seems to be affected both by natural and anthropogenic sources. As observed in Figure 10, the low amplitude time intervals observed at the SM band can be followed in the 1-10 Hz band for most of the stations, but the amplitude appears here more scattered. We have shown that some sites have a strong anthropogenic signature in this band. Therefore, we conclude that this is the frequency with a less clear dominant source, being affected by processes such as ocean swell, wind or rainfall, but also by human activities. The imprint of anthropogenic sources, evidenced by day/night and working days/weekends differences, but also by the changes in official time at spring and fall and, very often in Spain, by a break-off interval corresponding to lunch time, is stronger in the 10-20 Hz and tends to vanish at higher frequencies, for which the amplitude variation patterns strongly differ among stations.

The results of this study prove that a systematical analysis of the amplitude variations at different frequency bands can be useful for identifying the main sources of seismic noise affecting permanent networks, in particular in the case of such sources that vary over time. The PSD plots commonly used in quality control procedures, such as those shown in Figure 2, typically do not allow the user to locate short term periods of increased noise. Besides, they usually mask differences between day/night and weekend/working days that may be relevant to evaluate if a certain site is strongly affected by anthropic noise and has to be moved to an alternative location

The interest of the study is double fold; on the one hand, the analysis of a large number of stations over a full year period provides new constraints on the analysis of the dominant sources of noise at different frequency bands. On the other hand, this study makes it possible to identify stations affected by specific sources of noise during episodic time intervals. The analysis also makes it possible to evaluate the degree of seismic noise affecting each station, and more specifically, its variation over time. This seems particularly useful at high frequencies, where background noise can prevent the automatic identification of the arrival of seismic waves generated by weak local earthquakes.

Further advances will include the inspection of the horizontal components, with specific attention to eventual tilting variations, as well as the study of the accelometric network deployed recently. Also, efforts based on the use of machine learning strategies can be made to automatically identify special features, such as those discussed in Section 5.3, avoiding eventual misinterpretations of the data and allowing the network managers to decide if any action should be taken. From a methodological point of view, we encourage the use of the SeismoRMS package for routine quality checking procedures carried out systematically by the seismic network managers.

Acknowledgements

We acknowledge the GEO3BCN-CSIC LabSis Laboratory (http://labsis.geo3bcn.csic.es, last accessed: 08 May 2024) for providing their signal processing capacities for this contribution. We are grateful to Mario Ruiz, technical director of Labsis, for fruitful discussions on seismic noise. This work has benefited from partial support of the EPYSIM Project, funded by the Spanish Ministry of Science and Innovation (Ref.: PID2022-136981NB-I00).

7 Data and code availability

The seismic dataset used in this study, is publicly distributed through the Institut Cartogràfic i Geològic de Catalunya (ICGC) EIDA Data Center (last accessed: 11 March 2024). The SeismoRMS code is publicly available in a Zenodo repository (Lecocq et al., 2020).

8 Competing interests

The authors declare no competing financial interests.

References

Alexopoulos, J. D., Dilalos, S., Voulgaris, N., Gkosios, V., Giannopoulos, I.-K., Kapetanidis, V., and Kaviris, G. The Contribution of Near-Surface Geophysics for the Site Characterization of Seismological Stations. *Applied Sciences*, 13(8):4932, Apr. 2023. doi: 10.3390/app13084932.

Ashkenazy, Y. and Yizhaq, H. The diurnal cycle and temporal trends of surface winds. *Earth and Planetary Science Letters*, 601:117907, Jan. 2023. doi: 10.1016/j.epsl.2022.117907.

Bromirski, P. D., Duennebier, F. K., and Stephen, R. A. Mid-ocean microseisms. *Geochemistry, Geophysics, Geosystems*, 6(4), Apr. 2005. doi: 10.1029/2004gc000768.

Diaz, J., Ruiz, M., Udina, M., Polls, F., Martí, D., and Bech, J. Monitoring storm evolution using a high-density seismic network. *Scientific Reports*, 13(1), Feb. 2023. doi: 10.1038/s41598-023-28902-8.

Díaz, J. On the origin of the signals observed across the seismic spectrum. *Earth-Science Reviews*, 161:224–232, Oct. 2016. doi: 10.1016/j.earscirev.2016.07.006.

Díaz, J., Ruiz, M., Sánchez-Pastor, P. S., and Romero, P. Urban Seismology: on the origin of earth vibrations within a city. *Scientific Reports*, 7(1), Nov. 2017. doi: 10.1038/s41598-017-15499-y.

Díaz, J., Ruiz, M., Curto, J. J., Torta, J. M., Ledo, J., Marcuello, A., and Queralt, P. On the observation of magnetic events on broad-band seismometers. *Earth, Planets and Space*, 72(1), July 2020. doi: 10.1186/s40623-020-01236-9.

Hasselmann, K. A statistical analysis of the generation of microseisms. *Reviews of Geophysics*, 1(2):177–210, May 1963. doi: 10.1029/rg001i002p00177.

Institut Cartogràfic i Geològic de Catalunya. Catalan Seismic Network [Data set]. *International Federation of Digital Seismograph Networks*, 1984. doi: 10.7914/SN/CA.

Kozlovskaya, E. and Kozlovsky, A. Influence of high-latitude geomagnetic pulsations on recordings of broadband force-balanced seismic sensors. *Geoscientific Instrumentation, Methods and Data Systems*, 1(2):85–101, Aug. 2012. doi: 10.5194/gi-1-85-2012.

Krischer, L., Megies, T., Barsch, R., Beyreuther, M., Lecocq, T., Caudron, C., and Wassermann, J. ObsPy: a bridge for seismology into the scientific Python ecosystem. *Computational Science & Discovery*, 8(1):014003, May 2015. doi: 10.1088/1749-4699/8/1/014003.

Lecocq, T., Massin, F., Satriano, C., Vanstone, M., and Megies, T. SeismoRMS - A simple Python/Jupyter Notebook package for studying seismic noise changes, Version 1.0, 2020. doi: 10.5281/ZENODO.3820046.

Longuet-Higgins, M. S. A theory of the origin of microseisms. *Philosophical Transactions of the Royal Society of London. Series A, Mathematical and Physical Sciences*, 243(857):1–35, 1950. doi: http://dx.doi.org/10.1098/rsta.1950.0012.

Nakamura, Y. A method for dynamic characteristics estimation of subsurface using microtremor on the ground surface. *Railway Technical Research Institute, Quarterly Reports*, 30(1), 1989.

Peterson, J. R. *Observations and modeling of seismic background noise*. 1993. doi: 10.3133/ofr93322.

Rindraharisaona, E. J., Réchou, A., Fontaine, F. R., Barruol, G., Stamenoff, P., Boudevillain, B., Rigaud-Louise, F., and Delcher, E. Seismic Signature of Rain and Wind Inferred From Seismic Data. *Earth and Space Science*, 9(10), Oct. 2022. doi: 10.1029/2022ea002328.

Stephen, R. A., Spiess, F. N., Collins, J. A., Hildebrand, J. A., Orcutt, J. A., Peal, K. R., Vernon, F. L., and Wooding, F. B. Ocean Seismic Network Pilot Experiment. *Geochemistry, Geophysics, Geosystems*, 4(10), Oct. 2003. doi: 10.1029/2002gc000485.

Welch, P. The use of fast Fourier transform for the estimation of power spectra: A method based on time averaging over short, modified periodograms. *IEEE Transactions on Audio and Electroacoustics*, 15(2):70–73, June 1967. doi: 10.1109/tau.1967.1161901.

Wilgus, J. T., Ringler, A. T., Schmandt, B., Wilson, D. C., and Anthony, R. E. Background Seismic Noise Levels among the Caribbean Network and the Role of Station Proximity to Coastline. *Seismological Research Letters*, 95(4):2141–2152, Mar. 2024. doi: 10.1785/0220230215.